

Dark Matter in Inert Triplet Models

Takeshi Araki^{1,*}, C. Q. Geng^{2,3,†} and Keiko I. Nagao^{2‡}

¹*Institute of High Energy Physics, Chinese Academy of Sciences, Beijing 100049, China*

²*Department of Physics, National Tsing Hua University, Hsinchu, Taiwan 300*

³*National Center for Theoretical Sciences, Hsinchu, Taiwan 300*

We study the inert triplet models, in which the standard model (SM) is extended to have a new $SU(2)_L$ triplet scalar ($Y=0$ or 2) with an Z_2 symmetry. We show that the neutral component of the triplet can be a good dark matter candidate. In particular, for the hypercharge $Y=0$ triplet model, the WMAP data favors the region where the dark matter mass is around 5.5 TeV, which is also consistent with the direct detection experiments. In contrast, for the $Y=2$ model, although dark matter with its mass around 2.8 TeV is allowed by WMAP, it is excluded by the direct detection experiments because the spin-independent cross section is enhanced by the Z mediated tree-level scattering process.

I. INTRODUCTION

From the Wilkinson Microwave Anisotropy Probe (WMAP) observation, the relic abundance of the cold dark matter in the universe is determined to be [1]

$$\Omega_{CDM}h^2 = 0.1123 \pm 0.0035, \quad (1)$$

where $h = 0.710 \pm 0.025$ is the scaled current Hubble parameter in units of $100 \text{ km sec}^{-1} \text{ Mpc}^{-1}$. Since the standard model (SM) cannot accommodate dark matter, new physics is expected. In this paper, we study dark matter in a model containing an $SU(2)_L$ triplet scalar with the hypercharge $Y=0$ or 2 under $U(1)_Y$, which is clearly one of the minimal extensions of the SM. In the model, the triplet is odd under an Z_2 symmetry so that it neither directly couples to the SM fermions nor develops a vacuum expectation value (VEV). We will refer to the model as the inert triplet model (ITM). Since the neutral component of the triplet scalar can be the lightest one and stable in both $Y=0$ and 2 cases, it is a good dark matter candidate.

It can be shown that there are three and five new parameters in the $Y=0$ and 2 ITMs, which are the same as those in the inert singlet and doublet models [2–5]¹, respectively. Clearly, the $Y=0$ ITM is one of the minimal inert models.

Besides the relic abundance, the direct searches of dark matter also provide constraints on new physics models. For the spin-independent (SI) cross section, one has that

$$\sigma_{SI} \lesssim 5 \times 10^{-44} - 10^{-42} \text{ cm}^2 \quad (2)$$

for the range of the Weakly Interacting Massive Particle (WIMP) mass smaller than 10^3 GeV [6]. Note that if the dark matter mass is larger, the constraint in Eq. (2) will be relaxed.

The paper is organized as follows. In Sec. II, we introduce the ITM of the $Y=0$ case and discuss the relic abundance as well as the direct detection of dark matter. We extend our study to the $Y=2$ ITM in Sec. III. We conclude in Sec. IV.

II. DARK MATTER IN $Y=0$ ITM

A. Basic framework

In addition to the SM particles, we introduce an $SU(2)_L$ triplet scalar with $Y=0$ and impose an Z_2 symmetry in which the triplet is assigned to be odd and the others even. Furthermore, we assume that the triplet scalar does not develop the VEV to keep the Z_2 symmetry unbroken. The relevant Lagrangian is given by

$$\begin{aligned} \mathcal{L} &= |D_\mu H|^2 + \text{tr}|D_\mu T|^2 - V(H, T), \\ V(H, T) &= m^2 H^\dagger H + M^2 \text{tr}[T^2] + \lambda_1 |H^\dagger H|^2 \\ &\quad + \lambda_2 (\text{tr}[T^2])^2 + \lambda_3 H^\dagger H \text{tr}[T^2], \end{aligned} \quad (3)$$

where D_μ is the covariant derivative and the doublet H and triplet T scalars are defined as

$$H = \begin{pmatrix} \phi^+ \\ \frac{1}{\sqrt{2}}(h + i\eta) \end{pmatrix}, \quad T = \begin{pmatrix} \frac{1}{\sqrt{2}}T^0 & -T^+ \\ -T^- & -\frac{1}{\sqrt{2}}T^0 \end{pmatrix}, \quad (4)$$

with $\langle h \rangle = v = 246$ GeV and $\langle T^0 \rangle = 0$, respectively. In order to assure the stability of the potential, we require the conditions

$$\lambda_1, \lambda_2 > 0, \quad 2\sqrt{\lambda_1 \lambda_2} > |\lambda_3| \quad \text{for negative } \lambda_3. \quad (5)$$

The potential in Eq. (3) becomes a local minimum if and only if

$$m^2 < 0, \quad 2M^2 + \lambda_3 v^2 > 0, \quad (6)$$

where $v^2 = -m^2/\lambda_1$. After h acquires the VEV, the scalars gain the following masses:

$$m_h^2 = 2\lambda_1 v^2, \quad m_{T^0}^2 = m_{T^\pm}^2 = M^2 + \frac{1}{2}\lambda_3 v^2. \quad (7)$$

* araki@ihep.ac.cn

† geng@phys.nthu.edu.tw

‡ nagao@phys.nthu.edu.tw

¹ In [5], the ITM was also mentioned.

Note that η and ϕ^\pm are the massless Nambu-Goldstone bosons eaten by the SM gauge fields. Although the masses of T^0 and T^\pm are degenerate at the tree level, a small mass splitting

$$m_{T^\pm} = m_{T^0} + (166 \text{ MeV}) \quad (8)$$

will appear once the radiative corrections [4] are taken into account. Hence, T^0 turns out to be the lightest component of the triplet scalar and moreover, it is stable due to Z_2 .

B. Oblique parameters and Higgs boson mass

Since the triplet scalar is added to the SM, one may think that it affects the so-called oblique (S and T) parameters. In general, however, an $Y=0$ triplet has no contribution to the S parameter, while the contribution to the T parameter is also vanishing in the limit of $m_{T^0} = m_{T^\pm}$ [7]. Even if we consider the mass splitting in Eq. (8), its effect is negligibly small. Therefore, the constraint on the Higgs boson mass (m_h) from the precision electroweak measurements is the same as that in the SM. In our calculation, we restrict m_h to be within the range of

$$114 \text{ GeV} < m_h < 185 \text{ GeV} \quad (9)$$

as estimated in Ref. [8] with the excluded region of 158 ~ 175 GeV reported by the Tevatron [9].

C. W and Z decay widths and DM mass

Since the decay widths of Z and W precisely measured by the LEP and Tevatron, agree well with the SM predictions, the new decay processes $W^\pm \rightarrow T^\mp T^0$ and $Z \rightarrow T^\pm T^\mp$ must be strongly suppressed. To this end, we impose the following condition:

$$m_{T^0} - (166 \text{ MeV}) > m_Z/2. \quad (10)$$

D. Relic Abundance

We now examine the thermal relic abundance of T^0 . The evolution of the number density of T^0 is obtained by solving the Boltzmann equation

$$\frac{dn_{T^0}}{dt} + 3Hn_{T^0} = -\langle\sigma v_{T^0}\rangle(n_{T^0}^2 - n_{T^0,eq}^2), \quad (11)$$

where H is the Hubble parameter, v_{T^0} stands for relative velocity of T^0 , $\langle\cdots\rangle$ represents the thermal average of a function in brackets, and n_{T^0} , $n_{T^0,eq}$ and σ are the number density, the number density in thermal equilibrium and the total annihilation cross section of T^0 , respectively. In the model, since the mass splitting between dark matter (T^0) and charged components (T^\pm) is much

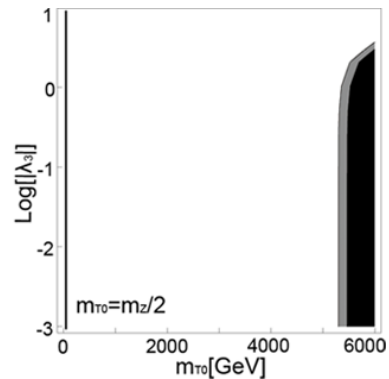


FIG. 1. Relic abundance for $m_h = 120$ GeV with the vertical axis of $\text{Log}[\lambda_3]$, where black, gray, and white regions show the parameter regions larger than, agreed with, and smaller than the WMAP constraint, respectively, while the straight line indicates the LEP bound for T^0 .

smaller than their masses, the coannihilation effects of $T^0 T^\pm$ and $T^\pm T^\mp$ should be included in σ [10].

In Fig. 1, we show the relic abundance of T^0 , where we have used *micrOMEGAS 2.4* [11] to scan the parameter λ_3 from 10^{-3} to 10. For small couplings, i.e. $\lambda_3 \lesssim 1$, the dark matter annihilation is governed by the weak interaction. So the annihilation cross section does not decrease so much. In this case, the main (co)annihilation modes are $T^0 T^\pm \rightarrow \gamma W^\pm$, $T^0 T^0 \rightarrow W^+ W^-$ and $T^+ T^- \rightarrow W^+ W^-$. On the other hand, in the large coupling region (i.e. $\lambda_3 \gtrsim 1$), the main annihilation modes are $T^0 T^0 \rightarrow t\bar{t}$ and $T^0 T^0 \rightarrow hh$. Although some of those annihilation are mediated by the Higgs h , the relic abundance is not subject to m_h so much as long as we take $m_h = 114 \sim 185$ GeV. Since the trilinear coupling of h involves only λ_3 (see Eq. (3)), the cross sections are enhanced. Note that the relic abundance depends on only λ_3 , whereas both λ_1 and λ_2 are irrelevant to the annihilation interactions. From the figure, we find that for $5.4 \text{ TeV} \lesssim m_{T^0} \lesssim 6 \text{ TeV}$, the relic abundance agrees with the WMAP data in Eq. (1). We remark that $m_{T^0} \lesssim 5000$ GeV is allowed if there are some other dark matter sources.

E. Direct Detection

The SI cross section of the $Y=0$ ITM is shown in Fig. 2. From the figure, we can see that in most of the region, the model escapes the constraint from the direct search. We note that the contribution of the SI cross section is insensitive to m_h as long as $114 \text{ GeV} \leq m_h \leq 185 \text{ GeV}$ even though it comes from the T^0 -quark and T^0 -gluon collisions through the $T^0 - T^0 - h$ coupling. Since the T^0 -quark (u,d) scattering has a small cross section due to the small Yukawa couplings, while T^0 -gluon scattering occurs only in loop level, the SI cross section is clearly suppressed.

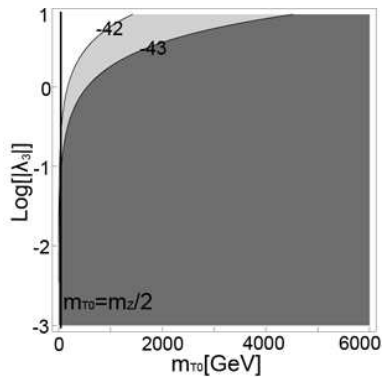


FIG. 2. Spin-independent scattering cross section between the dark matter T^0 and nucleus particles, where numbers on lines represent the cross sections in cm^2 unit, while light gray and dark gray regions are allowed by direct searches of dark matter.

III. DARK MATTER IN Y=2 ITM

A. Basic framework

In the model with the inert triplet scalar of Y=2, the Z_2 invariant scalar potential is given by

$$V(H, T) = m^2 H^\dagger H + M^2 \text{tr}[T^\dagger T] + \lambda_1 |H^\dagger H|^2 + \lambda_2 \text{tr}[T^\dagger T T^\dagger T] + \lambda_3 (\text{tr}[T^\dagger T])^2 + \lambda_4 H^\dagger H \text{tr}[T^\dagger T] + \lambda_5 H^\dagger T T^\dagger H, \quad (12)$$

where

$$T = \begin{pmatrix} \frac{1}{\sqrt{2}} T^+ & T^{++} \\ T_r^0 + iT_i^0 & -\frac{1}{\sqrt{2}} T^+ \end{pmatrix}. \quad (13)$$

The masses of the scalars are calculated as

$$\begin{aligned} m_h^2 &= 2\lambda_1 v^2, \\ m_{T_r^0}^2 &= m_{T_i^0}^2 = M^2 + \frac{1}{2}(\lambda_4 + \lambda_5)v^2, \\ m_{T^\pm}^2 &= M^2 + \frac{1}{2}\left(\lambda_4 + \frac{\lambda_5}{2}\right)v^2 = m_{T_r^0(T_i^0)}^2 - \frac{\lambda_5}{4}v^2, \\ m_{T^{\pm\pm}}^2 &= M^2 + \frac{1}{2}\lambda_4 v^2 = m_{T_r^0(T_i^0)}^2 - \frac{\lambda_5}{2}v^2. \end{aligned} \quad (14)$$

We note that, in order to make T_r^0 and T_i^0 to be the lightest Z_2 -odd particles, we take $\lambda_5 < 0$ afterward.

B. Relic abundance

The total relic abundance of T_r^0 and T_i^0 is shown² in Fig. 3. Note that the masses of T^\pm and $T^{\pm\pm}$ are auto-

² Here, we again use *micrOMEGAS* and assume that the interactions of T_r^0 and T_i^0 are the same, which simplifies our calculation to the relic abundance of T_r^0 only. It is justified since the interactions of T_r^0 and T_i^0 are almost the same.

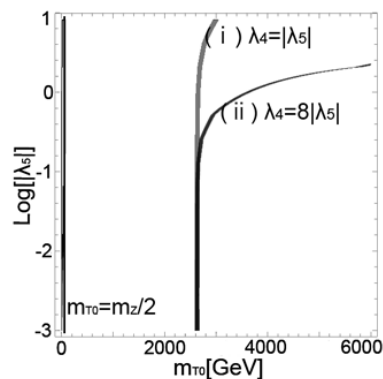


FIG. 3. Relic abundance of Y=2 ITM for $m_h = 120$ GeV, where gray regions are the parameter regions agreed with WMAP and the right (left) handed sides of the gray regions correspond to the regions larger (smaller) than the observation.

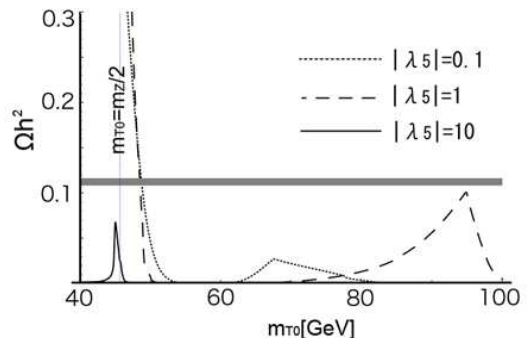


FIG. 4. Relic abundance in the Y=2 ITM for the small m_{T^0} region with $m_h = 120$ GeV, where the light gray region is allowed by WMAP.

matically fixed if m_{T^0} and λ_5 are known. It is easy to see that the relic abundance tends to be large compared to that in the Y=0 case. Moreover, the mass splitting among the triplet scalars is not so small unless the absolute value of $|\lambda_5|$ is enormously small. Since coannihilations of the triplet scalars are not so effective, the relic abundance gets enhanced. However, in the small λ_5 region (i.e., $|\lambda_5| \lesssim 1$), the masses of T_r^0 , T^+ and T^{++} are still degenerate. As the result, the coannihilation involving T^+ and T^{++} (e.g., $T^+ T^{--} \rightarrow \gamma W^-$ and $T^+ T^- \rightarrow W^+ W^-$) is active. In the large $|\lambda_5|$ region, as the mass degeneracy of the triplet components is lifted, the coannihilation effect becomes weaker, which enhances the relic abundance. However, the annihilation cross section becomes large due to the large couplings of λ_4 and $|\lambda_5|$, which suppresses the relic abundance more effective than the coannihilation effect.

In the region with $m_{T^0} \lesssim 100$ GeV, the relic abundance drastically changes due to the resonance effect as well as the opening of new annihilation final states. We show the relic abundance in the small mass region in Fig. 4. In the

figure, we have fixed $\lambda_4 = |\lambda_5|/8$. For $|\lambda_5| = 10$, the relic abundance tends to be small due to the large coupling. The main annihilation mode is $T_r^0 T_r^0 (T_i^0 T_i^0) \rightarrow b\bar{b}$, while $T_r^0 T_r^0 (T_i^0 T_i^0) \rightarrow Zh$ is also effective if $m_{T_r^0}$ is large. For $|\lambda_5| = 1$, we find that the relic abundance suddenly decreases at $m_{T_r^0} \sim 60$ GeV and $m_{T_r^0} \sim 100$ GeV due to $T_r^0 T_r^0 (T_i^0 T_i^0) \rightarrow h \rightarrow b\bar{b}$ and $T_r^0 T_r^0 (T_i^0 T_i^0) \rightarrow hh$, respectively. In contrast, for $|\lambda_5| = 0.1$, the main interaction mode at the large $m_{T_r^0}$ region is $T_r^0 T_r^0 (T_i^0 T_i^0) \rightarrow W^+ W^-$ since the gauge interaction is more effective than the Higgs interaction. In this case, the relic abundance becomes much smaller. For a smaller $|\lambda_5|$ (i.e. $|\lambda_5| = 0.01$), the figure is similar to that for the case of $|\lambda_5| = 10$ as the relic abundance is small due to the large coannihilation cross section of $T^- T^{++} \rightarrow \gamma W^+$, $T_r^0 (T_i^0) T^+ \rightarrow \gamma W^+$ and $T_r^0 (T_i^0) T^+ \rightarrow ZW^+$. We note that for $\lambda_4 = |\lambda_5|$, the figures are similar to those with $|\lambda_5| = \lambda_4/8 = 0.1$ and 0.01 since the main interactions enhanced by the large Higgs coupling are proportional to $(\lambda_4 + \lambda_5)$.

In the region with $|\lambda_4|/|\lambda_5| \neq 1$, where $T_r^0 T_r^0 (T_i^0 T_i^0) \rightarrow hh$ is most effective, the relic abundance is reduced. In the case of $|\lambda_4|/|\lambda_5| = 1$, the tri-Higgs couplings proportional to $(\lambda_4 + \lambda_5)$ are canceled to be 0. Since the effective couplings of the Higgs bosons are very weak, the relic abundance is determined by gauge interactions.

We comment on the direct detection of the Y=2 case. Unlike Y=0, there are three scattering processes in the Y=2 model. Two of them are the same as those in the Y=0 case, while the other one is the T^0 -quark scattering through the gauge coupling of T^0 to Z as shown explicitly in Appendix. The latter has a larger cross section due to the gauge coupling. Because of this large cross section, almost all region is excluded by the direct detection constraint in Eq. (2)³. In particular, we have checked that in all of the regions allowed by LEP experiments, the SI cross section is larger than about 10^{-37}cm^2 . Therefore, even if the ratio of λ_4 and λ_5 (i.e., the coupling of DM-gluon scattering) is changed, the cross section is still larger than the constraint from the direct detection.

IV. CONCLUSION

We have studied dark matter in the two inert triplet models. In the Y=0 model, we have shown that the favored region by the WMAP result is around $m_{T^0} \sim 5.5$ TeV based on the relic abundance. On the other hand, since T^0 scatters quarks only for the small Yukawa couplings as it does not couple to Z at the Lagrangian level, while the T^0 -gluon scattering occurs at loop level, dark matter (T^0) in most of the regions, including that favored by WMAP, is allowed from the

direct detection. For the Y=2 case, $m_{T^0} \sim 2.8$ TeV is preferred in terms of the relic abundance of T^0 . However, since the T^0 -quark scattering is allowed at tree level due to the $T^0 - Z$ coupling, which enhances the scattering cross section, most of the regions is excluded by the direct detection.

Acknowledgement We are grateful to G. Bélanger and A. Pukhov for their kind help for *micrOMEGAs*. The work of T.A. was supported in part by the National Natural Science Foundation of China under Grant No. 10425522 and No. 10875131. C.Q.G. and K.I.N were partially supported by the National Science Council of Taiwan under Grant No. NSC-98-2112-M-007-008-MY3 and the National Tsing Hua University under the Boost Program No. 97N2309F1.

V. APPENDIX: INTERACTIONS

We expand Eqs. (3) and (12) in terms of the component fields to show specific scalar and gauge interactions of the triplet. In the followings, we will use the following definitions of the gauge fields:

$$D_\mu = \partial_\mu - ig \left[W_\mu^a \frac{\sigma^a}{2}, \right] - ig' \frac{Y}{2} B_\mu \quad (15)$$

$$W_\mu^\pm = \frac{1}{\sqrt{2}} (W_\mu^1 \mp iW_\mu^2), \quad (16)$$

$$Z_\mu = c_w W_\mu^3 - s_w B_\mu, \quad A_\mu = s_w W_\mu^3 + c_w B_\mu, \quad (17)$$

where $\sigma^{a=1\cdots 3}$ are the Pauli matrices, $s_w(c_w) = \sin(\theta_w(\cos \theta_w))$, and θ_w is the weak mixing angle.

A. Interactions in Y=0 ITM

The scalar interactions:

- $m^2 H^\dagger H = m^2 [|\phi^+|^2 + \frac{1}{2}(h^2 + \eta^2)]$,
- $M^2 \text{tr}[T^2] = M^2 [2|T^+|^2 + (T^0)^2]$,
- $\lambda_1 |H^\dagger H|^2 = \lambda_1 [|\phi^+|^2 + \frac{1}{2}(h^2 + \eta^2)]^2$,
- $\lambda_2 (\text{tr}[T^2])^2 = \lambda_2 [2|T^+|^2 + (T^0)^2]^2$,
- $\lambda_3 H^\dagger H \text{tr}[T^2]$
 $= [|\phi^+|^2 + \frac{1}{2}(h^2 + \eta^2)] [2|T^+|^2 + (T^0)^2]$.

The three-point gauge interactions:

- $2ig [(\partial^\mu T^+) W_\mu^- T^0 + (\partial^\mu T^0) W_\mu^+ T^-] + h.c.$,
- $2ig(\partial^\mu T^+)(c_w Z_\mu + s_w A_\mu) T^- + h.c.$,

and four-point gauge interactions:

- $g^2 [|W_\mu^- T^+ - W_\mu^+ T^-|^2 + 2|W_\mu^+ T^0|^2]$,

³ The DM-DM-Z coupling tends to make the SI cross section beyond the constraint of the direct search, which is consistent with the result in Ref. [12]

- $2g^2(c_w Z_\mu + s_w A_\mu)^2 |T^+|^2$,
- $2g^2(W_\mu^+ T^0)(c_w Z_\mu + s_w A_\mu) T^- + h.c. .$

Notice T^0 does not couple to Z boson in this model.

B. Interactions in Y=2 ITM

The scalar interactions:

- $M^2 \text{tr}[T^\dagger T] = M^2 \left[|T^{++}|^2 + |T^+|^2 + T_r^{02} + T_i^{02} \right]$,
- $\lambda_2 \text{tr}[T^\dagger T T^\dagger T]$
 $= \lambda_2 \left[\frac{1}{2} |T^+|^4 + |T^{++}|^4 + (T_r^{02} + T_i^{02})^2 \right.$
 $\left. + 2|T^+|^2 (T_r^{02} + T_i^{02}) + 2|T^+|^2 |T^{++}|^2 \right.$
 $\left. - \{T^- T^{++} T^- (T_r^0 + iT_i^0) + h.c.\} \right]$,
- $\lambda_3 (\text{tr}[T^\dagger T])^2$
 $= \lambda_3 \left[|T^{++}|^2 + |T^+|^2 + T_r^{02} + T_i^{02} \right]^2$,
- $\lambda_4 H^\dagger H \text{tr}[T^\dagger T]$
 $= \lambda_4 \left[|\phi^+|^2 + \frac{1}{2}(h^2 + \eta^2) \right]$
 $\times \left[|T^{++}|^2 + |T^+|^2 + T_r^{02} + T_i^{02} \right]$,
- $\lambda_5 H^\dagger T T^\dagger H$
 $= \lambda_5 \left[\frac{1}{2} |\phi^+|^2 |T^+|^2 + \frac{1}{2}(h^2 + \eta^2)(T_r^{02} + T_i^{02}) \right.$
 $\left. + |\phi^+|^2 |T^{++}|^2 + \frac{1}{4}(h^2 + \eta^2) |T^+|^2 \right.$
 $\left. + \frac{1}{2} \{ \phi^- T^+ (T_r^0 - iT_i^0)(h + i\eta) \}$

$$- \phi^- T^{++} T^- (h + i\eta) + h.c. \}].$$

The three point gauge interactions:

- $ig \left[(\partial^\mu T^+) (W_\mu^- (T_r^0 - iT_i^0) - W_\mu^+ T^{--}) \right.$
 $\left. - (\partial^\mu T^{++}) W_\mu^- T^- \right.$
 $\left. + (\partial^\mu T_r^0 + i\partial^\mu T_i^0) W_\mu^+ T^- \right] + h.c. ,$
- $i[(gc_w - g's_w)Z_\mu + 2gs_w A_\mu] (\partial^\mu T^{++}) T^{--} + h.c. ,$
- $\frac{4m_Z}{v} [-(\partial^\mu T_r^0) T_i^0 + (\partial^\mu T_i^0) T_r^0] Z_\mu ,$
- $ig' (-s_w Z_\mu + c_w A_\mu) (\partial^\mu T^+) T^- + h.c. ,$

and four-point gauge interactions:

- $g^2 \left[|W_\mu^+|^2 (T_r^{02} + T_i^{02}) \right.$
 $\left. + |W_\mu^+|^2 |T^{++}|^2 + 2|W_\mu^+|^2 |T^+|^2 \right]$,
- $\frac{4m_Z^2}{v^2} Z^\mu Z_\mu (T_r^{02} + T_i^{02}) ,$
- $[(g^2 - g'^2)(c_w^2 - s_w^2) Z_\mu Z^\mu + 4g^2 s_w^2 A_\mu A^\mu$
 $+ 4gg'(c_w^2 - s_w^2) Z_\mu A^\mu] |T^{++}|^2$,
- $[(-g^2 c_w + 2gg's_w) Z^\mu - 3g^2 s_w A^\mu]$
 $\times T^{++} W_\mu^- T^- + h.c. ,$
- $[(-g^2 c_w - 2gg's_w) Z^\mu + g^2 s_w A^\mu]$
 $\times (T_r^0 + iT_i^0) W_\mu^+ T^- + h.c. ,$
- $g'^2 (s_w^2 Z^\mu Z_\mu + c_w^2 A^\mu A_\mu - 2s_w c_w Z_\mu A^\mu) |T^+|^2$.

Unlike Y=0 case, both T_r^0 and T_i^0 couple to Z boson.

-
- [1] E. Komatsu *et al.*, arXiv:1001.4538 [astro-ph.CO].
- [2] V. Silveira and A. Zee, Phys. Lett. B**161**, 136 (1985); C. P. Burgess, M. Pospelov and T. ter Veldhuis, Nucl. Phys. B**619**, 709 (2001); W. L. Guo and Y. L. Wu, JHEP **1010**, 083 (2010).
- [3] E. Ma, Phys. Rev. D**73**, 077301 (2006); R. Barbieri, L. J. Hall and V. S. Rychkov, Phys. Rev. D**74**, 015007 (2006); L. Lopez Honorez *et al.*, JCAP **0702**, 028 (2007); E. Lundstrom, M. Gustafsson and J. Edsjo, Phys. Rev. D**79**, 035013 (2009); P. Agrawal, E. M. Dolle and C. A. Krenke, Phys. Rev. D**79**, 015015 (2009); S. Andreas, M. H. G. Tytgat and Q. Swillens, JCAP **0904**, 004 (2009); E. Nezri, M. H. G. Tytgat and G. Vertongen, JCAP **0904**, 014 (2009); E. M. Dolle and S. Su, Phys. Rev. D**80**, 055012 (2009); C. Arina, F. S. Ling and M. H. G. Tytgat, JCAP **0910**, 018 (2009); E. Dolle *et al.*, Phys. Rev. D**81**, 035003 (2010); X. Miao, S. Su and B. Thomas, Phys. Rev. D**82**, 035009 (2010); L. Lopez-Honorez and C. E. Yaguna, arXiv:1011.1411 [hep-ph].
- [4] M. Cirelli and A. Strumia, New J. Phys. **11**, 105005 (2009).
- [5] T. Hambye *et al.*, JHEP **0907**, 090 (2009) [Erratum-ibid. **1005**, 066 (2010)].
- [6] J. Angle *et al.* [XENON Collaboration], Phys. Rev. Lett. **100**, 021303 (2008); Z. Ahmed *et al.* [The CDMS-II Collaboration], Science **327**, 1619 (2010).
- [7] H. H. Zhang, W. B. Yan and X. S. Li, Mod. Phys. Lett. A**23**, 637 (2008).
- [8] See <http://lepewwg.web.cern.ch/LEPEWWG/>.
- [9] Tevatron New Phenomena and Higgs Working Group, <http://tevnpnphwg.fnal.gov/>.
- [10] K. Griest and D. Seckel, Phys. Rev. D**43**, 3191 (1991); S. Mizuta and M. Yamaguchi, Phys. Lett. B**298**, 120 (1993).
- [11] G. Belanger *et al.*, arXiv:1004.1092 [hep-ph].
- [12] E. J. Chun, JHEP **0912**, 055 (2009).